Solar Energy
And Sustainable Development
Refereed, biannual scientific journal issued by:
The Libyan Center for Solar Energy Research and Studies

Study of the Gravimetric, Electronic and Thermoelectric Properties of $XAlH_3$ (X = Be, Na, K) as hydrogen storage perovskite using DFT and the BoltzTrap Software Package

Ayoub Koufi[1]*, Younes Ziat[2], Hamza Belkhanchi[3].

[1,2,3]Engineering and Applied Physics Team (EAPT), Superior School of Technology, Sultan Moulay Slimane University, Beni Mellal, Morocco
[1,2,3]The Moroccan Association of Sciences and Techniques for Sustainable Development (MASTSD), Beni Mellal, Morocco.

E-*mail:* [1] ayoub.koufi@usms.ma , [2] dr-matter@gmx.fr .

SPECIAL ISSUE ON:

The 2024 1st International Conference on Materials Sciences and Mechatronics for Sustainable Energy and the Environment
October 1-3, 2024 at Béni-Mellal, Morocco

KEYWORDS

Electrical; DFT; Gravimetric; Merit factor; $XAlH_3$.

ABSTRACT

In the context of density functional theory (DFT), this study examines the structural, electronic, gravimetric and thermoelectric properties of perovskite compounds $XAlH_3$ (X = Be, Na and K) using the generalized gradient approximation (GGA). Calculations were performed with the BoltzTrap software package integrated into the Wien2k code, enabling analysis of total energy and atomic volume using the Murnaghan equation of state.

The results show that the materials behave like conductors due to the overlap of the conduction band and the valence band, with a zero band gap. $NaAlH_3$ and $KAlH_3$ show increasing electrical and thermal conductivity with temperature, while $BeAlH_3$ exhibits non-linear behavior, peaking at 400 K. These results suggest that $XAlH_3$ materials are promising for hydrogen storage applications and thermoelectric devices, underlining their potential to support a sustainable hydrogen economy.

*Corresponding author.

DOI: https://doi.org/10.51646/jsesd.v14iSI_MSMS2E.403

دراسة الخواص الوزنية والإلكترونية والحرارية لـ $XAlH_3$ (X=Be, Na, K) باعتباره بيروفسكايت لتخزين الهيدروجين باستخدام DFT و برامج BoltzTrap

أيوب كوفي، يونس زيات، حمزة بلخنشي.

ملخص: في سياق نظرية الكثافة الوظيفية (DFT)، تبحث هذه الدراسة في الخصائص الهيكلية والإلكترونية والجاذبية والحرارية لمركبات البيروفسكايت $XAlH_3$ (X = Be وNa وK) باستخدام تقريب التدرج المعمم (GGA). تم إجراء الحسابات باستخدام حزمة برامج BoltzTrap المدمجة في كود Wien2k، مما يتيح تحليل إجمالي الطاقة والحجم الذري باستخدام معادلة مورناغان للحالة. أظهرت النتائج أن المواد تتصرف مثل الموصلات بسبب تداخل نطاق التوصيل ونطاق التكافؤ، مع وجود فجوة نطاق صفر. يُظهر $NaAlH_3$ و $KAlH_3$ زيادة في التوصيل الكهربائي والحراري مع درجة الحرارة، بينما يُظهر $BeAlH_3$ سلوكًا غير خطي، ويبلغ ذروته عند 400 كلفن. وتشير هذه النتائج إلى أن مواد $XAlH_3$ واعدة لتطبيقات تخزين الهيدروجين والأجهزة الكهروحرارية، مما يؤكد قدرتها على دعم اقتصاد الهيدروجين المستدام.

الكلمات المفتاحية – كهربائية ؛ تجهيز الدوائر؛ الجاذبية؛ عامل الجدارة؛ $XAlH_3$.

1. INTRODUCTION

The most abundant elements on Earth, carbon and hydrogen play a fundamental role in the field of energy. Hydrogen, in particular, stands out for its exceptional energetic properties [1, 2]. When it reacts with oxygen, it generates considerably more heat than traditional energy sources, while producing no CO2, given the absence of carbon in the reaction [3, 4]. This makes hydrogen a clean, renewable and particularly efficient energy carrier, making it an essential component of sustainable energy solutions [5, 6]. Thanks to these properties, hydrogen is already used in a variety of fields, including vehicle fuel cells, power generation, internal combustion engines and Ni-MH batteries, commonly used in hybrid vehicles [7, 8]. However, despite its undeniable advantages, hydrogen faces two major obstacles to widespread adoption: large-scale production and storage [9, 10]. At present, the production of hydrogen in massive quantities relies on processes that are either expensive or not very environmentally friendly, such as steam methane reforming or electrolysis fueled by non-renewable energy sources. Therefore, for hydrogen to become a viable alternative to fossil fuels, it is crucial to develop more efficient, less costly and more environmentally-friendly production methods [11, 12]. At the same time, hydrogen storage represents a major technical challenge [13, 14]. Because of its low volumetric energy density, it has to be stored under high pressure, at very low temperatures, or in the form of chemical compounds, which gives rise to technical complications and safety risks [15, 16]. It is therefore imperative to improve storage technologies to make the use of hydrogen safe, efficient and economically viable. To overcome these challenges, an integrated approach combining hydrogen with other alternative energy sources, such as wind, nuclear and solar, is essential [17, 18]. This strategy would not only reduce our dependence on fossil fuels, but also fully exploit the environmental and energy benefits of hydrogen, thus contributing to a more sustainable energy future [19, 20]. Hydrogen, with its exceptional energy properties, is an ideal candidate for sustainable energy solutions. However, the challenges associated with its production and storage call for innovative approaches. This is where perovskite hydrides show particular promise. Thanks to their unique ability to store large quantities of hydrogen, these crystalline materials offer a potential answer to current limitations in hydrogen storage, enabling the full potential of this clean energy carrier to be exploited [21, 22]. By exploring the properties of these perovskites and using advanced methods such as density functional theory (DFT), it becomes possible to optimize their performance for more sustainable and efficient energy applications. In this context, perovskite hydrides are proving to be key materials for meeting the challenges associated with hydrogen storage. The

flexible, tunable crystal structure of perovskites, based on the ABX3 composition, gives them a unique ability to store large quantities of hydrogen. This storage capacity is facilitated by the incorporation of hydride ions into the crystal lattice, enabling the reversible absorption and release of hydrogen. This mechanism makes hydride perovskites ideal candidates for sustainable energy solutions [23, 24]. Experimental investigations have shown that compounds such as $NaMgH_3$ and $KMgH_3$ possess promising hydrogen storage capabilities when synthesized under high pressure and temperature [25] [26]. In addition, studies of $MgXH_3$ compounds (X = Cr, Fe, Mn, Co, Cu, Ni) have revealed that these materials are not only thermodynamically stable, but also exhibit favorable properties such as positive phonon dispersion frequencies [27, 28].
What's more, the synergy between hydride ions and perovskite structures adds catalytic functions that could advance electrochemical and photoelectrochemical processes, essential for new energy conversion technologies [29, 30]. Density functional theory (DFT) methods have been widely used to explore the structural, electrical, and optical properties of perovskite compounds [31, 32, 33, 34]. By modeling perovskites at the atomic scale, researchers can anticipate characteristics such as electrical conductivity, thermal conductivity, Seebeck coefficient and thermoelectric merit factor [35, 36, 37]. These advances pave the way for the development of materials with optimal thermoelectric properties, contributing to more sustainable and efficient thermal energy conversion technologies. The importance of perovskite hydrides as high-capacity energy storage materials is amplified by advances in the analysis of their electronic and thermoelectric properties. To better understand the electronic and thermoelectric properties of perovskite hydrides, we use the BoltzTrap software package within the framework of density functional theory (DFT), applying the generalized gradient approximation (GGA). This approach enables us to analyze in detail the electronic characteristics and thermoelectric performance of $XAlH_3$ compounds (X = Be, Na, and K). The following sections will present the computational methods employed, outline the results obtained, and discuss conclusions regarding the temperature and thermoelectric properties of these materials. The aim is to determine how these properties influence the potential of hydrides for energy storage and thermal conversion applications, and to optimize their use in sustainable energy technologies.

2. CALCULATION METHOD

The present study focuses on evaluating the hydrogen storage capacities and other important properties of $XAlH_3$ (X = Be, K, and Na) using theoretical calculations based on density functional theory (DFT). The generalized gradient approximation (GGA) was employed to model exchange and correlation potentials, which is crucial for obtaining accurate results. Before analyzing the electronic and thermoelectric properties, an essential step was to optimize the crystal lattice volume to ensure that the structure studied was in its state of minimum energy stability. This optimization was carried out using the Birch-Murnaghan equation of state, integrated into the Wien2k code [38, 39]. To ensure the accuracy of the calculations, total energy and charge convergence during the self-consistent cycle (SCF) were rigorously controlled, with thresholds of 0.0001 Ry for total energy and 0.001(e) for charge. The Brillouin zone was densely sampled using a 10×10×10 k-point mesh, with octahedral integration. Subsequently, the thermoelectric properties were analyzed using the BoltzTrap software package, which models the electronic characteristics required for in-depth performance evaluation of $XAlH_3$ compounds.

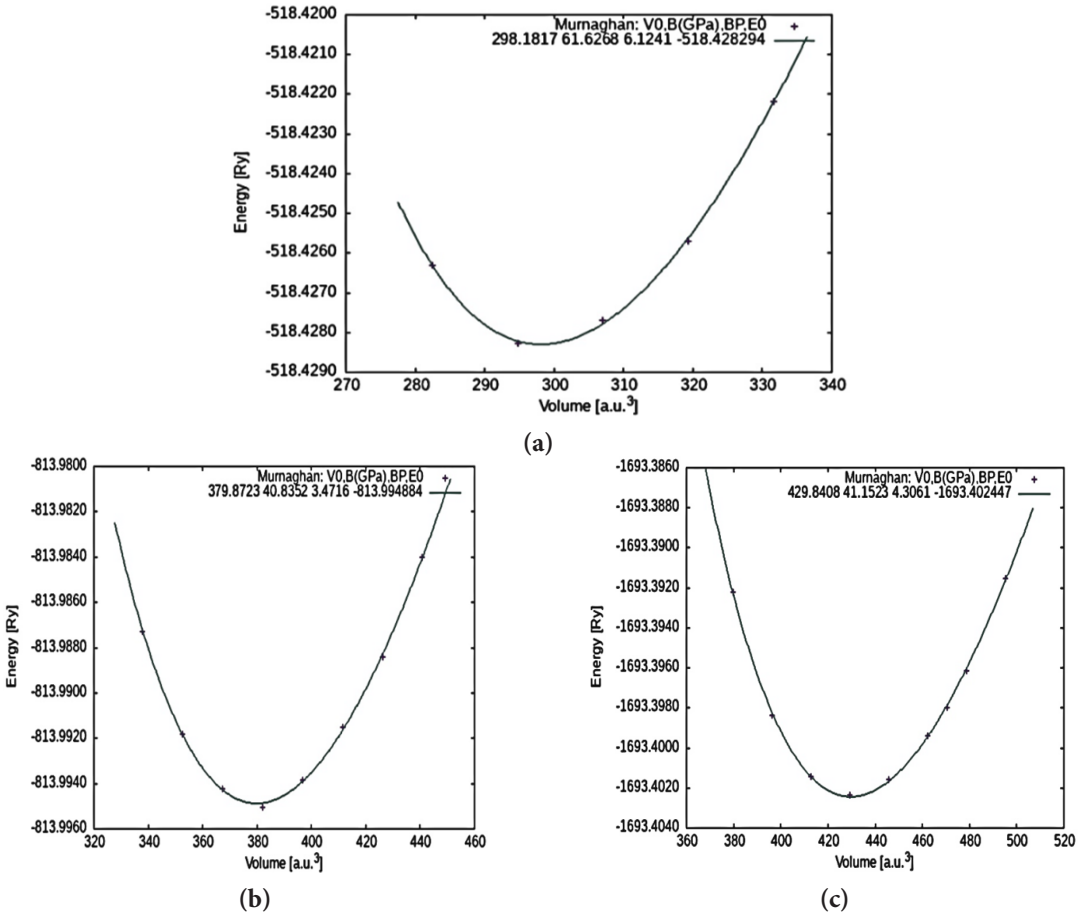

Figure 1. Variation of total energy as a function of volume for: a) $BeAlH_3$ and b) $NaAlH_3$ c) $KAlH_3$.

The Murnaghan equation of state is a mathematical relationship used to describe the behavior of materials under pressure, in particular the variation in volume of a substance as a function of applied pressure [31]. It is a simplified and often-used version of the equation of state, which expresses the relationship between volume, pressure and energy in a given system. This equation is particularly useful in simulations based on density functional theory (DFT) to optimize the crystal structure of a material. The postulated equilibrium lattice constants are obtained by fitting the total energy as a function of the normalized volume to the Murnaghan equation of state (EOS). The equilibrium lattice parameters (a_0) that we estimated reasonably agree with the experimental ones. By using the Birch-Murnaghan depression, the volumes extracted as a function of the predicted energies are displayed in Figure 1.

$$E = E_0 + \frac{B_0}{B_0'}(V - V_0)\frac{B_0 V_0}{B_0'(1 - B_0')}\left[\left(\frac{V}{V_0}\right)^{1-B_0'} - 1\right] \qquad (1)$$

P represents the pressure applied to the material, while V denotes the volume of the material under this pressure. The term V_0 corresponds to the initial volume, i.e. the volume at zero pressure. Parameter B is the isostatic compressibility modulus (or bulk modulus), which quantifies the material's resistance to compression. Finally, B_0' is the derivative of the compressibility modulus with respect to pressure, indicating how the compressibility modulus evolves as a function of the applied pressure. Where E is taken as the minimum energy, which is the ground state energy corresponding to the volume V_0 of the unit cell.

3. RESULTS AND DISCUSSION

3.1. Structural properties

The $XAlH_3$ compounds (X = Be, Na and K) are hydride perovskites whose structure is defined by the arrangement of atoms in a crystal lattice. In this configuration, the X atoms (Be, Na and K) occupy the corners of the unit cell (0, 0, 0), while the aluminum atoms (Al) are located in the center of the cell (1/2, 1/2, 1/2). The three hydrogen atoms are positioned on octahedral sites at the center of the cell faces (0, 1/2, 1/2), (1/2, 0, 1/2), and (1/2, 1/2, 0). The space group associated with this structure is $Pm\bar{3}m$ (No. 221). The lattice parameters of these compounds, as illustrated in Table 1, confirm the accuracy of the calculations and the reliability of the data obtained, in agreement with the results reported in previous studies [40, 41]. Figure 2 shows a representation of this crystal configuration, highlighting the regular arrangement of atoms and their role in the structural stability of $XAlH_3$ (X = Be, Na and K) hydrides.

Table 1. Theoretical and optimized lattice parameters.

Element	Lattice parameter (Other Study)	Lattice parameters optimize (Present Study)
$BeAlH_3$	a0=b0=c0= 3.57 Å [40]	a0=b0=c0= 3.5353 Å
$NaAlH_3$	a0=b0=c0= 3.792 Å [41]	a0=b0=c0= 3.8325 Å
$KAlH_3$	a0=b0=c0= 3.938 Å [41]	a0=b0=c0= 3.9936 Å

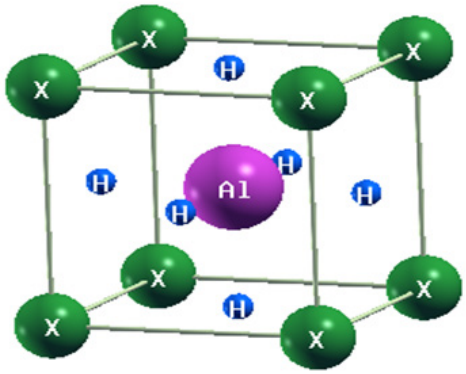

Figure 2. Structure of $XAlH_3$ (X = Be, Na, and K).

The analysis indicates that the gravimetric sizes and formation energies of $XAlH_3$ compounds (X = Be, Na, and K) decrease as the atomic number of the element increases. This trend is clearly illustrated in Figure 3, which shows that larger atomic volumes correspond to lower gravimetric sizes and formation energies [42, 43]. $BeAlH_3$, with a gravity size of 0.0761 $m.s^{-2}$ and an energy of formation of -518.42829 Ry, involves beryllium with an atomic number of 4. When we move on to $NaAlH_3$, where sodium has an atomic number of 11, the gravity size decreases to 0.0537 $m.s^{-2}$, and the energy of formation drops to -813.99488 Ry. This reduction in both parameters reflects the relationship between atomic size and the energy required for various processes, such as ionization and atomic bonding. The larger atomic radius and increased shielding effect in heavier elements such as potassium (K), with an atomic number of 19, contribute to this observed trend. This suggests that $BeAlH_3$ is relatively softer than the less flexible $KAlH_3$. As shown in Figure 4, there could be a correlation between atomic number, volume and other properties that influence material characteristics, suggesting patterns observed with increasing atomic number.

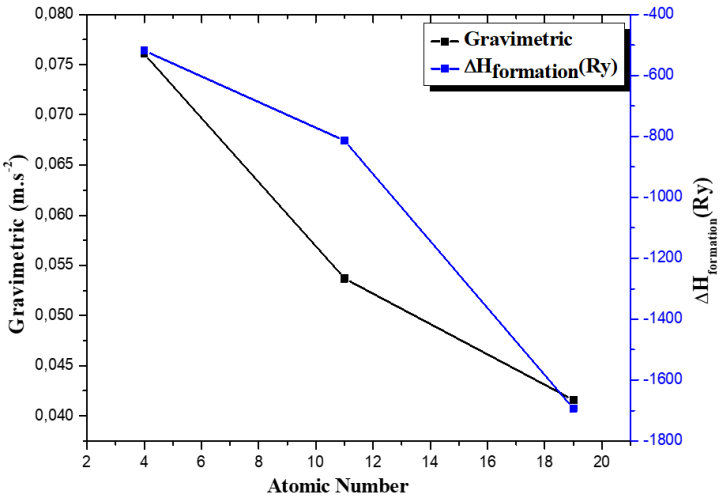

Figure 3. Gravimetric and $\Delta H_{formation}$ as a function of atomic number for $XAlH_3$ (X = Be, Na and K).

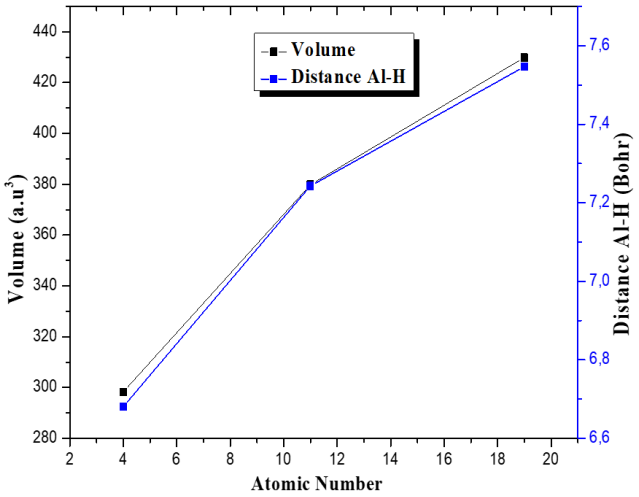

Figure 4. Volume and distance Al-H as a function of atomic number for $XAlH_3$ (X = Be, Na and K).

3.2. Electronic properties

The electronic properties of the perovskite-type hydrides $XAlH_3$ (X = Be, Na and K) have been calculated using the GGA method within the framework of density functional theory (DFT). These calculations are essential for understanding the electronic behavior of these materials and their potential applications. Figure 5 shows the band structures of these compounds, revealing a metallic character, as evidenced by the crossings between the conduction band minima (CB) and valence band maxima (VB) above the Fermi level (EF), set at 0 eV. This metallic behavior is also confirmed by analysis of the partial density of states (PDOS), shown in Figure 6. The results indicate that the s state of X (Be, Na and K) dominates the valence band contribution (VB) in the range from -12 to -6 eV, with notable contributions from the s states of H, s of X (Be, Na and K) and p of Al close to the EF in all cases. Hybridization between the X (Be, Na and K) s, H, and Al p states near the EF also contributes to this metallic behavior. Interestingly, metallic materials such as the perovskite hydrides studied here are particularly effective for hydrogen storage. Their high conductivity facilitates efficient charge transfer during hydrogen uptake and release processes, making them promising candidates for hydrogen storage applications [44]. However, the electronic properties of $XAlH_3$ compounds, combining band structure and density of states, underline their potential as efficient metallic materials for technological applications, particularly in hydrogen storage [45].

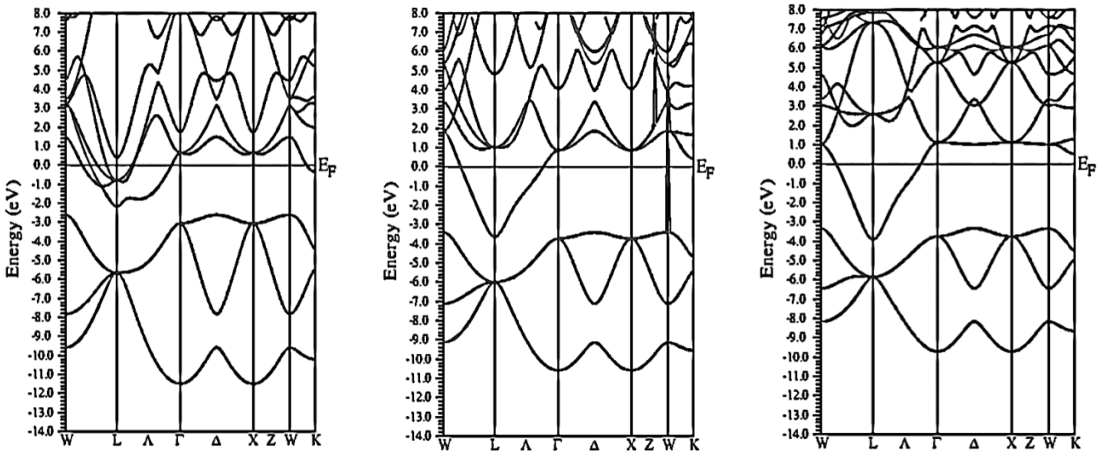

(a) (b) (c)

Figure 5. Band Structures of: a) $BeAlH_3$, b) $NaAlH_3$ and c) $KAlH_3$.

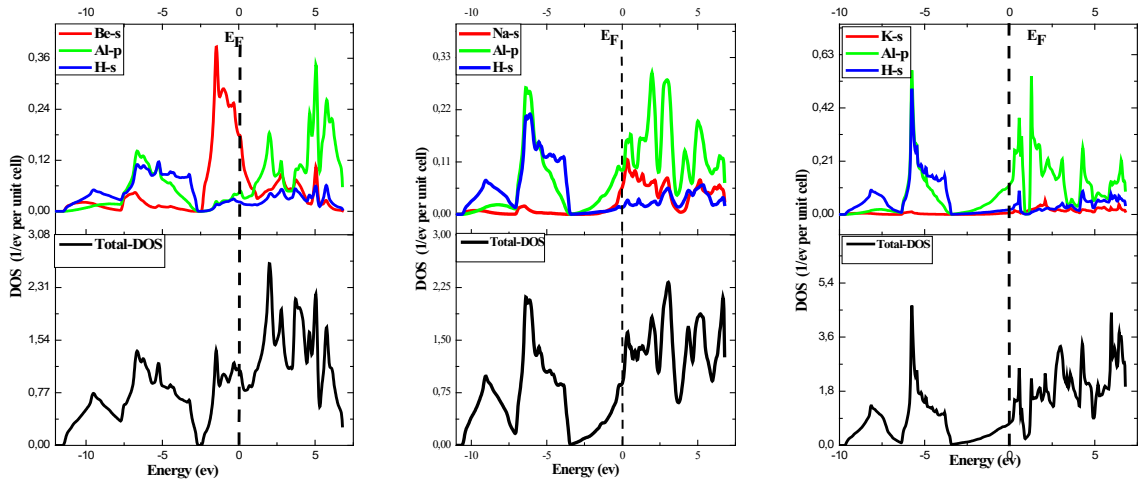

(a) (b) (c)

Figure 6. DOS of a) $BeAlH_3$, b) $NaAlH_3$, and c) $KAlH_3$.

3.3. Thermoelectrical Properties

The thermoelectric properties of $XAlH_3$ (X = Be, Na, and K) compounds are essential for assessing their effectiveness as materials for converting thermal energy into electricity, particularly in renewable energy systems where thermal energy is often wasted. The electron band structure, calculated using semi-classical Boltzmann transport theory and the rigid band theory implemented in the Boltz-Trap software package, plays a decisive role in the behavior of electron transport properties. The Seebeck coefficient (S), electrical conductivity (σ), and thermal conductivity (κ) were analyzed for these compounds, as they directly influence the material's merit factor (Zt), a key indicator of thermoelectric performance. The relationship between electrical and thermal conductivity, crucial for the efficiency of thermoelectric devices [46], was examined at temperatures ranging from 300 to 900K. A high Seebeck coefficient, combined with optimized thermal conductivity, suggests good potential for $XAlH_3$ materials in waste heat recovery applications. The combination of these properties enables us to determine the merit factor (Zt) and power factor (PF), which assess the overall performance of the materials under a variety of thermal conditions.

The electrical conductivity of perovskite $XAlH_3$ (X = Be, Na, and K) is a crucial aspect in understanding its potential for thermoelectric applications. Electrical conductivity, defined

by the flux of free charge carriers, depends on several factors, including the composition of the material, its crystalline structure, and the presence of impurities or imperfections in the lattice. These elements directly influence charge carrier mobility and, consequently, electrical conductivity. Figure 7 shows that the electrical conductivity of $BeAlH_3$ exhibits a non-linear trend, increasing between 300 and 400 K, then decreasing beyond this temperature range. In contrast, for $NaAlH_3$ and $KAlH_3$, electrical conductivity increases continuously with rising temperature, reaching respective maximum values of $3.50x10^{20}$ and $3.25x10^{20}$ W/(K.m.s). This difference in behavior between the compounds can be attributed to the variation in crystal structure and electronic interactions specific to each X element (Be, Na, K). The temperature dependence of electrical conductivity suggests that these materials may exhibit variable performance depending on conditions of use. In addition, the pressure and temperature conditions under which these materials are evaluated can modify their electronic properties, thus influencing electrical conductance. However, an increase in temperature can lead to an increase in charge carrier mobility in some cases, while in others it can cause scattering effects or carrier recombination that reduce conductivity. These observations highlight the importance of thorough characterization of $XAlH_3$ materials to optimize their use in thermoelectric devices or other applications requiring stable and predictable electrical conductivity.

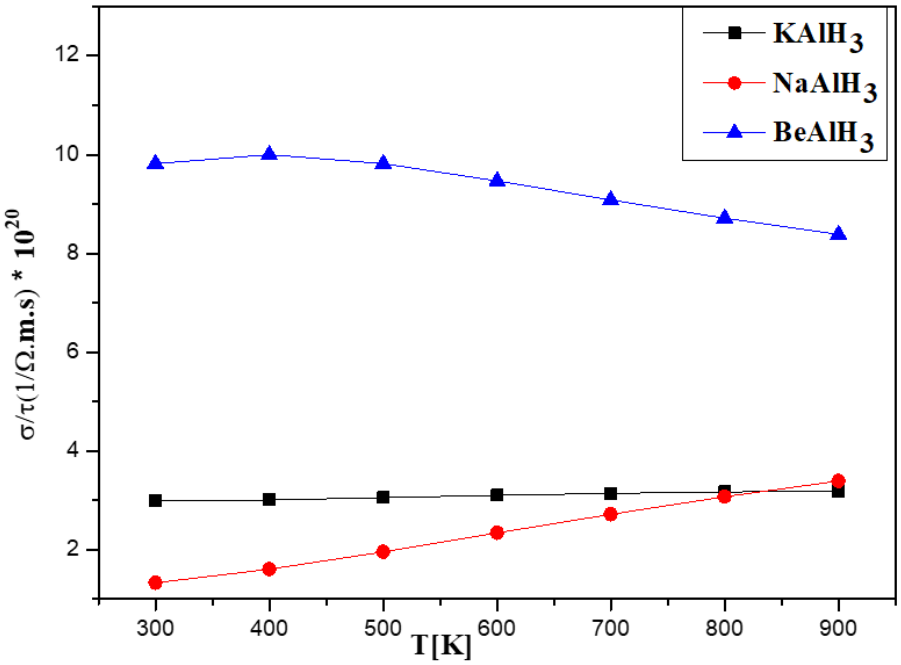

Figure 7. Electrical Conductivity $XAlH_3$ (X = Be, Na and K).

The thermal conductivity of $XAlH_3$ (X = Be, Na, and K) is a key factor in assessing their effectiveness in thermoelectric applications, as it determines heat transfer through the material. Thermal conductivity, shown in Figure 8, shows a linear increase with temperature for all three compounds studied. At 900 K, thermal conductivity reaches values of $11.8x10^{15}$ W/(K.m.s) for $BeAlH_3$, $14x10^{15}$ W/(K.m.s) for $NaAlH_3$, and $6.10x10^{15}$ W/(K.m.s) for $KAlH_3$. This behavior can be explained by the vibrations of free electrons in the material, which increase with temperature. As the temperature rises, the thermal vibrations of the atoms intensify, increasing heat transfer. In $XAlH_3$ compounds, this increase in molecular vibrations is directly linked to the rise in temperature, which explains the observed increase in thermal conductivity. The significance of these results lies in the fact that, for thermoelectric applications, too high a thermal conductivity can be unfavorable, as it leads to rapid heat dissipation, thus reducing the efficiency of thermal-to-electrical energy conversion. Therefore, although the increase in thermal conductivity with

temperature is an expected and well-documented phenomenon, finding a balance between thermal and electrical conductivity is essential to maximize the efficiency of $XAlH_3$-based thermoelectric devices. The variations observed between $BeAlH_3$, $NaAlH_3$, and $KAlH_3$ also show the influence of different atomic compositions on the thermal behavior of these materials, suggesting that selection of the appropriate compound X could optimize performance for specific applications.

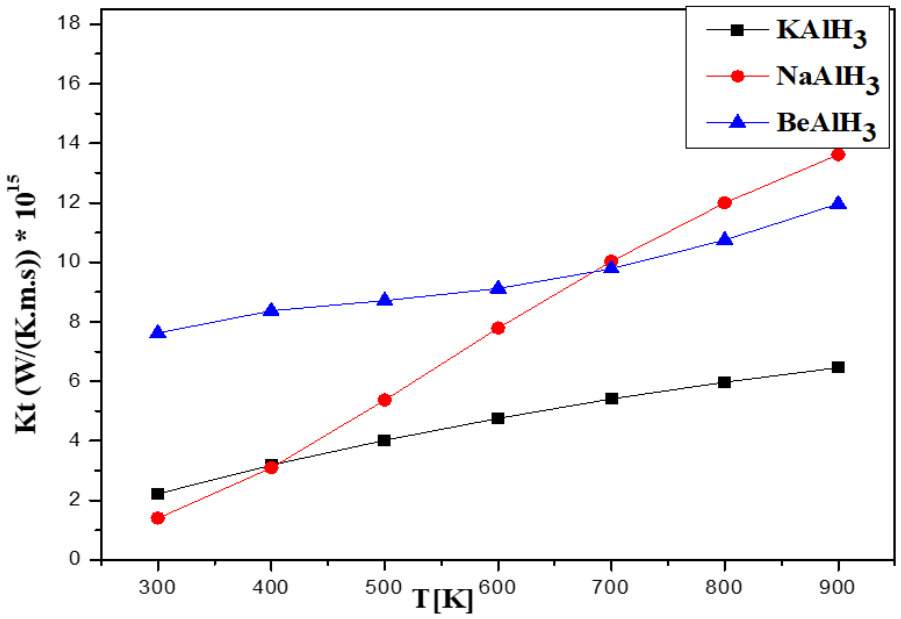

Figure 8. Thermal Conductivity of $XAlH_3$ (X = Be, Na and K).

The thermoelectric merit factor (Zt) is a key measure of a material's efficiency in thermoelectric applications. It represents the ratio between the efficiency of thermal-to-electrical energy conversion and the material's ability to maintain this conversion [46]. The following equation explains the merit factor (Zt):

$$Zt = \frac{\sigma s^2 T}{\kappa} \qquad (2)$$

where σ is the electrical conductivity, T is the temperature, S is the Seebeck coefficient, and κ is the thermal conductivity [47].

Figure 9 illustrates Zt variations for $XAlH_3$ (X = Be, Na, and K) as a function of temperature. For $BeAlH_3$ and $KAlH_3$, Zt initially decreases between 300 and 400 K, but then increases between 400 and 900 K, reaching values of $2.5x10^{-2}$ and $7.5x10^{-2}$ respectively at 900 K. This behavior suggests that, although these materials are less efficient at lower temperatures, their efficiency improves considerably at higher temperatures. In contrast, for $NaAlH_3$, Zt decreases continuously with increasing temperature, reaching a value of $1.25x10^{-2}$ at 900 K. Notably, $NaAlH_3$ has a very high Zt of $29x10^{-2}$ at 300 K, making it a very efficient material at low temperatures, although its efficiency decreases with increasing temperature. These results show that the choice of the appropriate $XAlH_3$ material is highly dependent on the application's expected operating temperature. $NaAlH_3$ might be ideal for applications requiring high performance at low temperatures, while $BeAlH_3$ and $KAlH_3$ might be better suited to high-temperature environments where their efficiency increases. This differential behavior can be attributed to the intrinsic nature of each material, influenced by factors such as electronic structure, interatomic interactions, and thermal response. In summary, analysis of the Zt merit factor indicates that each $XAlH_3$ compound has distinct thermoelectric properties, with optimum performance at specific temperature ranges.

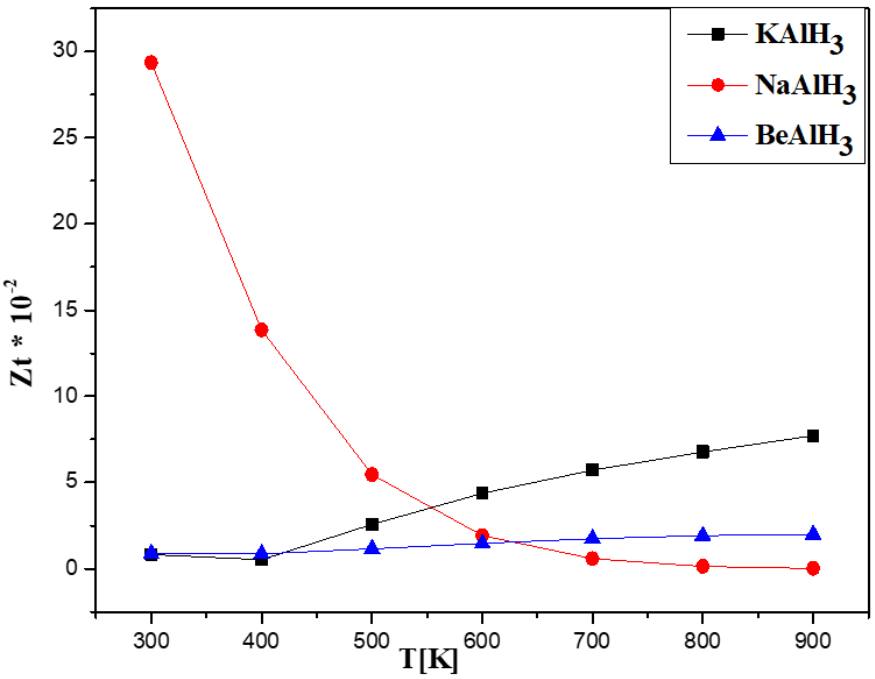

Figure 9. Merit Factor of $XAlH_3$ (X = Be, Na and K).

The power factor (PF) is another crucial measure for assessing a material's thermoelectric performance. It is directly related to the efficiency with which a material can convert thermal energy into electrical energy, taking into account both electrical conductivity and the Seebeck coefficient [46]. Materials with high power factors are sought after for energy generation, especially those with a power factor greater than unity, particularly in high-temperature thermoelectric industries. The PF is explained by the following equation:

$$Power\ factor\ (PF) = \sigma S^2 \qquad (3)$$

Figure 10 shows variations in the power factor for $XAlH_3$ (X = Be, Na, and K) as a function of temperature.

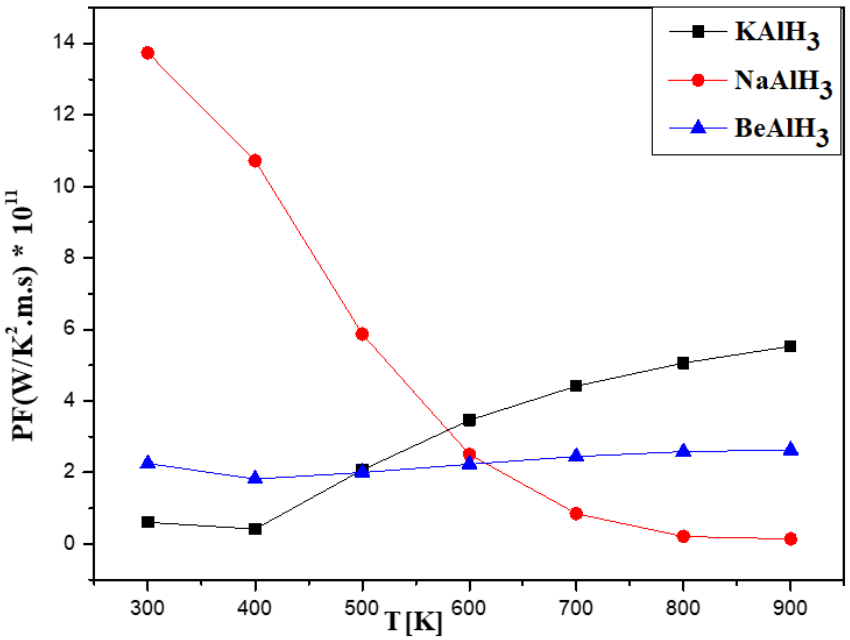

Figure 10. Power Factor of XAlH3 (X = Be, Na and K).

For $NaAlH_3$, the power factor decreases continuously with increasing temperature, indicating

that this material loses efficiency with increasing temperature. However, it has an exceptionally high value of $13.9x10^{11}$ W/(K^2.m.s) at 300 K, making it an excellent candidate for applications requiring high performance at low temperatures. In contrast, for $BeAlH_3$ and $KAlH_3$, the power factor initially decreases between 300 and 400 K, but then increases between 400 and 900 K, reaching values of $2.41x10^9$ W/(K^2.m.s) and $5.9x10^{11}$ W/(K^2.m.s) respectively at 900 K. This behavior suggests that these materials become more efficient at higher temperatures, which could make them more suitable for high-temperature environments.

4. CONCLUSION

In conclusion, this study used the BoltzTrap software package, integrated with the Wien2k code, to conduct an in-depth theoretical analysis of the structural, electrical and thermoelectric properties of $XAlH_3$ (X = Be, Na, and K) perovskite-type compounds. The results revealed that these compounds behave as conductors, characterized by an overlapping conduction band and valence band, with zero band gap, which is favorable for hydrogen storage applications. Thermoelectric properties, such as electrical conductivity, thermal conductivity, merit factor (Zt) and power factor (PF), showed that $BeAlH_3$ and $NaAlH_3$ are superior to $KAlH_3$ in several aspects, particularly in terms of performance at different temperatures. In addition, a trend was observed where formation energies and gravimetric sizes decrease with increasing atomic number of X elements, suggesting a correlation between atomic size and stability of these compounds. The successful integration of hydrogen storage technologies, supported by materials such as those studied here, will play a crucial role in the transition to a sustainable hydrogen economy. This will have important implications for applications in transport, energy storage and industrial processes. To accelerate progress in this field, it will be essential to continue investing in research, development and demonstration projects, while putting in place appropriate support policies and commercial incentives. The $XAlH_3$ compounds studied offer promising potential for various technological applications, thanks to their unique properties adapted to specific thermal conditions.

Author Contributions: Contribution to the conceptualization, methodology, investigation, and writing of the original draft. The author also reviewed and edited the manuscript for final approval.

Funding: The funding agency had no role in the design, data collection, analysis, or interpretation of the results.

Data Availability Statement: Not applicable.

Acknowledgments: The authors are warmly grateful to the support of "The Moroccan Association of Sciences and Techniques for Sustainable Development (MASTSD), Beni Mellal, Morocco," and to its president, professor Charaf Laghlimi, for the valuable proposals.

A special thank you to Professor Hanane Reddad from Sultan Moulay Slimane University, Beni Mellal, Morocco, for her technical and scientific support, as well as her full collaboration and discussion during the different steps of the present investigation.

Conflicts of Interest: The authors declare that they have no conflict of interest.

REFERENCES

[1] R. Šulc, & P. Ditl, A technical and economic evaluation of two different oxygen sources for a small oxy-combustion unit. Clea Prod, 309, 127427 (2021)

[2] Q. Xu, Z. Zou, Y. Chen, K. Wang, Z. Du, J. Feng, & Y. Xiong, Performance of a novel-type of heat flue in a coke oven based on high-temperature and low-oxygen diffusion combustion technology. Fuel,

267, 117160 (2020)

[3] G. Varvoutis, A. Lampropoulos, E. Mandela, M. Konsolakis, & G. E. Marnellos, Recent advances on CO2 mitigation technologies: on the role of hydrogenation route via green H2. Energies, 15(13), 4790 (2022)

[4] K. A. Trowell, S. Goroshin, D.L Frost, & J. M. Bergthorson, J. M. Aluminum and its role as a recyclable, sustainable carrier of renewable energy. Applied Energy, 275, 115112 (2020)

[5] C. Ghenai, M. Albawab, & M. Bettayeb, Sustainability indicators for renewable energy systems using multi-criteria decision-making model and extended SWARA/ARAS hybrid method. Renewable Energy, 146, 580-597 (2020)

[6] M. Majid, Renewable energy for sustainable development in India: current status, future prospects, challenges, employment, and investment opportunities. Ener. Sust. and Soc, 10(1), 1-36 (2020)

[7] V. Arun, R. Kannan, S. Ramesh, M. Vijayakumar, P. S. Raghavendran, M. Siva Ramkumar… & V. P. Sundramurthy, Review on Li-Ion Battery vs Nickel Metal Hydride Battery in EV. Advances in Mate. Sci. and Eng, 7910072 (2022)

[8] S. Arya, & S. Verma, Nickel-metal hydride (Ni-MH) batteries. Rechargeable Batteries: History, Prog. and Appli, 131-175 (2020)

[9] N. Sazali, Emerging technologies by hydrogen: A review. Hydrogen Energy, 45(38), 18753-18771 (2020)

[10] N. Ma, W. Zhao, W. Wang, X. Li, & H. Zhou, Large scale of green hydrogen storage: Opportunities and challenges. Hydrogen Energy, 50, 379-396 (2023)

[11] M. Aravindan, V. S. Hariharan, T. Narahari, A. Kumar, K. Madhesh, P. Kumar, & R. Prabakaran, Fuelling the future: A review of non-renewable hydrogen production and storage techniques. Rene. and Sust. Ene. Revi, 188, 113791 (2023)

[12] E. B. Agyekum, C. Nutakor, A. M. Agwa, & S. Kamel, A critical review of renewable hydrogen production methods: factors affecting their scale-up and its role in future energy generation. Membranes, 12(2), 173 (2022)

[13] B. Zhang, S. X. Zhang, R. Yao, Y. H. Wu, J. S. & Qiu, Progress and prospects of hydrogen production: Opportunities and challenges. Ele. Sci. and Tec , 19(2), 100080 (2021)

[14] X. Xu, Q. Zhou, & D. Yu, The future of hydrogen energy: Bio-hydrogen production technology. Hydrogen Energy, 47(79), 33677-33698 (2022)

[15] L. Van Hoecke, L. Laffineur, R. Campe, P. Perreault, S. W. Verbruggen, & S. Lenaerts, Challenges in the use of hydrogen for maritime applications. Ene. & Env. Sci, 14(2), 815-843 (2021)

[16] R. R. Ratnakar, N. Gupta, K. Zhang, C. van Doorne, J. Fesmire, B. Dindoruk, & V. Balakotaiah, Hydrogen supply chain and challenges in large-scale LH2 storage and transportation. Hydrogen Energy, 46(47), 24149-24168 (2021)

[17] A. N. Sosa, F. Santiago, Á. Miranda, A. Trejo & al. Alkali andtransition metal atom-functionalized germanene for hydrogen storage: A DFT investigation, Hydrogen Energy, 46, 20245-20256 (2021)

[18] L. Rtemi, W. El-Osta, and A. Attaiep, Hybrid System Modeling for Renewable Energy Sources, 12, 13–28 (2023)

[19] M. Usman, Hydrogen storage methods: Review and current status, Renew, 167, 112743 (2022)

[20] Y. Pan & Y. Ende, Theoretical prediction of structure, electronic and optical properties of VH2 hydrogen storage material, Hydrogen Energy, 47, 27608-27616 (2022)

[21] S. Y. Lee, J. H. Lee, Y. H. Kim, J. W. Kim, K. J. Lee, & S. J. Park, Recent progress using solid. State. Mate. for hyd. Sto : a short review. Processes, 10(2), 304 (2022)

[22] S. P. Filippov, & A. B. Yaroslavtsev, Hydrogen energy: Development prospects and materials. Russ. Che. Rev, 90(6), 627 (2021)

[23] M. K. Masood, W. Khan, K. Chaoui, Z. Ashraf, S. Bibi, A. Kanwal, ... & J. Rehman, Theoretical investigation of XSnH3 (X: Rb, Cs, and Fr) perovskite hydrides for hydrogen storage application. Hydrogen Energy, 63, 1248 (2024)

[24] M. Mohan, N. P. Shetti, & T. M. Aminabhavi, Perovskites: A new generation electrode materials for storage applications. Power Sources, 574, 233166 (2023)

[25] JA. Nunez, High-pressure and high-temperature synthesis of light perovskite hydrides for hydrogen storage. Universit´e Grenoble Alpes; (2022)

[26] K. Ikeda & al. Reversible hydriding and dehydriding reactions of perovskite-type hydride NaMgH3. Scripta. Mater 53(3), 319–22 (2005)

[27] U. Rehman, Zia, & al. A DFT study of structural, electronic, mechanical, phonon, thermodynamic, and H2 storage properties of lead-free perovskite hydride MgXH3 (X= Cr, Fe, Mn). Phy. and Che. Solids, 186, 11801 (2024)

[28] Z. Rehman, & al. Ab initio insight into the physical properties of MgXH3 (X= Co, Cu, Ni) lead-free perovskite for hydrogen storage application. Env. Sci. Poll. Cont. Ser, 30, 113889–113902 (2023)

[29] C. Xia, H. Wang, J. K. Kim, & J. Wang, Rational design of metal oxide-based heterostructure for efficient photocatalytic and photoelectrochemical systems. Adv. Fun. Mat, 31(12), 2008247 (2021)

[30] E. Mousset, & D. D. Dionysiou, Photoelectrochemical reactors for treatment of water and wastewater: a review. Env. Che. Let, 18(4), 1301-1318 (2020)

[31] M. Miri, Y. Ziat, H. Belkhanchi, & Y. A. El Kadi, The effect of pressure on the structural, optoelectronic and mechanical conduct of the XZnF3 (X= Na, K and Rb) perovskite: First-principles study. Mod. Phys. B, 2550096. (2024) https://doi.org/10.1142/S0217979225500961.

[32] A. Koufi, Y. Ziat, H. Belkhanchi, M. Miri, N. Lakouari, & F. Z. Baghli, A computational study of the structural and thermal conduct of MgCrH3 and MgFeH3 perovskite-type hydrides: FP-LAPW and BoltzTraP insight. In E3S Web of Conferences (Vol. 582, p. 02003) (2024). https://doi.org/10.1051/e3sconf/202458202003

[33] A. Bouzaid, Y. Ziat, H. Belkhanchi, H. Hamdani, A. Koufi, M. Miri, ... & Z. Zarhri, Ab initio study of the structural, electronic, and optical properties of MgTiO3 perovskite materials doped with N and P. In E3S Web of Conferences (Vol. 582, p. 02006) (2024). https://doi.org/10.1051/e3sconf/202458202006

[34] Z. Zarhri, A. D. Cano, O. Oubram, Y. Ziat, & A. Bassam, Optical measurements and Burstein Moss effect in optical properties of Nb-doped BaSnO3 perovskite. Micro & Nano. 166, 207223 (2022)

[35] F. A. Zhao, H. Y. Xiao, Z. J. Liu, S. Li, & X. T. Zu, A DFT study of mechanical properties, thermal conductivity and electronic structures of Th-doped Gd2Zr2O7. Acta Materialia, 121, 299-309 (2016)

[36] Y. Wang, Y. J. Hu, B. Bocklund, S. L. Shang, B. C. Zhou, Z. K. Liu, &. L. Q. Chen, First-principles thermodynamic theory of Seebeck coefficients. Physical. Review B, 98(22), 224101 (2018)

[37] M. Bürkle, T. J. Hellmuth, F. Pauly, & Y. Asai, First-principles calculation of the thermoelectric figure of merit for [2, 2] paracyclophane-based single-molecule junctions. Physical Review B, 91(16), 165419 (2015)

[38] P. Blaha, K. Schwarz, F. Tran, R. Laskowski, G. K. Madsen, & L. D. Marks. WIEN2k: An APW+ lo program for calculating the properties of solids. The Journal of chemical physics, 152(7) (2020). https://doi.org/10.1063/1.5143061.

[39] J. P. Perdew, k. Burke, M. Ernzerhof, Generalized gradient approximation made simple. Phys. Rev. Lett. 77(18), 3865 (1996). https://doi.org/10.1103/PhysRevLett.77.3865.

[40] W. Khan. Computational screening of BeXH3 (X: Al, Ga, and In) for optoelectronics and hydrogen storage applications. Mat. Sci. in Semic. Pro, 174, 108221 (2024)

[41] N. Xu, R. Song, J. Zhang, Y. Chen, S. Chen, Li, S., ... & W. Zhang, First-principles study on hydrogen storage properties of the new hydride perovskite XAlH3 (X= Na, K). Hydrogen. Energy, 60, 434-440 (2024)

[42] E. Ededet, H. Louis, U. G. Chukwu, T. O. Magu, A. E. Udo, S. A. Adalikwu, & A. S. Adeyinka, A. S. Ab Initio Study of the Effects of d-Block Metal (Mn, Re, Tc) Encapsulation on the Electronic, Phonon, Thermodynamic, and Gravimetric, Hydrogen Capacity of BaXH4 Hydride Perovskites. Electronic. Materials, 53(1), 250-264 (2024)

[43] H. H. Raza, G. Murtaza, S. Razzaq, & A. Azam, Improving thermodynamic properties and desorption temperature in MgH2 by doping Be: DFT study. Molecular Simulation, 49(5), 497-508 (2023)

[44] A. Siddique, A. Khalil, B. S. Almutairi, M. B. Tahir, M. Sagir, Z. Ullah, ... & M. Alzaid. Structures and hydrogen storage properties of AeVH3 (Ae= Be, Mg, Ca, Sr) perovskite hydrides by DFT calculations Hydr. Ene, 48(63), 24401-24411 (2023)

[45] B. P. Tarasov, P. V. Fursikov, A. A. Volodin, M. S. Bocharnikov, Y. Y. Shimkus, A. M. Kashin, ... & M. V. Lototskyy. Metal hydride hydrogen storage and compression systems for energy storage technologies. Hydr. Ene. , 46(25), 13647-13657 (2021)

[46] M.Yaseen, H. Ambreen, Remsha, Mehmood, I. Munawar, Nessrin, Kattan,T. Alshahrani, S. Noreen, A. Laref. Investigation of optical and thermoelectric properties of PbTiO3 under pressure, Physica B: Cond. Mat, 615, 412857 (2021).

[47] D. Chang-Hao, D. Zhi-Fu, D. Zhong-Ke D, P. Hui & al. XMoSiN (X=S, Se, Te): A novel 2D Janus semiconductor with ultra-high carrier mobility and excellent thermoelectric performance, Europhysics Letters, 143, 16002 (2023).